

ON THE KNEE OF GALACTIC COSMIC RAYS IN LIGHT OF SUB-TeV SPECTRAL HARDENINGS

YI-QING GUO^{1,2} AND QIANG YUAN¹¹Key Laboratory of Dark Matter and Space Astronomy, Purple Mountain Observatory, Chinese Academy of Sciences, Nanjing 210008, Jiangsu, China; yuanq@pmo.ac.cn²Key Laboratory of Particle Astrophysics, Institute of High Energy Physics, Chinese Academy of Sciences, Beijing 100049, China*Draft version January 26, 2017*

ABSTRACT

More than fifty years after the discovery of the knee in the cosmic ray spectra, its physical origin remains a mystery. This is partly due to the ambiguity of the energy spectrum of individual composition. Recently, direct measurements from several balloon/satellite-borne detectors found significant spectral hardenings of cosmic ray nuclei at a few hundred GV rigidities. A joint modeling of the direct and indirect measurements of the cosmic ray spectra may help to understand the experimental systematics and probably the physics of the knee. In this work, we update the phenomenological “poly-gonato” model of the knee to include the spectral hardenings, with a changing spectral index of $\gamma + \beta \cdot \log E$ with respect to energy. We find that there is some tension between the direct and indirect measurements. Specifically, the hard spectra of CREAM suggest a relatively low energy cutoff of the individual cosmic ray spectrum around the knee, which is inconsistent with the light component spectra of the air shower measurements. Furthermore, the light component data from AS γ /ARGO-YBJ/WFCTA/KASCADE are consistent with the all-particle spectra. We expect that more precise measurements of the cosmic ray spectrum of individual composition at TeV energies and beyond by the operating space detectors such as CALET and DAMPE, and the ground based experiments such as LHAASO, will eventually solve these discrepancies. Finally, as an illustration, we show that a spatial-dependent diffusion under two-halo model is able to reproduce the results of this “modified poly-gonato” model.

1. INTRODUCTION

Nearly sixty years after the discovery of the knee in the cosmic ray (CR) spectra (Kulikov & Kristiansen 1958), its underlying physical mechanism is still under debate (Hörandel 2004). It is generally accepted that each composition has its own knee and the superposition of all compositions gives the observed break of the all-particle spectra at ~ 4 PeV. This is the so-called “poly-gonato” model (Hörandel 2003). The energy of the knee of each composition may be proportional to charge (Z -dependent) or atomic number (A -dependent), which can be used to probe the physical mechanism of the knee (Hörandel 2004). For example, the acceleration limit or propagation leakage may predict a Z -dependence of the knee of each composition (Lagage & Cesarsky 1983; Voelk & Biermann 1988; Ptuskin et al. 1993; Berezhko 1996; Wiebel-Sooth et al. 1998). On the other hand, an A -dependence may imply an interaction origin of the knee (Karakula & Tkaczyk 1993; Kazanas & Nicolaidis 2001; Candia et al. 2002; Hu et al. 2009; Wang et al. 2010; Guo et al. 2013).

The energy spectrum of individual nuclei composition is crucial to understand the knee puzzle. Many efforts have been paid to measure the individual spectrum with air shower experiments, however, no consensus has been achieved yet, primarily due to the systematical uncertainties of the absolute energy calibration. Some progresses in the spectral measurements of individual composition in PeV energies have been made in recent years with ground-based experiments. Although these measurements themselves are not completely consistent with each other, they may commonly suggest a knee below PeV for the light components (Huang & for the Tibet AS γ Collaboration 2013; Apel et al. 2013; Mari et al. 2015; Bartoli et al. 2015b; D’Amone et al. 2015; Montini & Mari 2016). Compared with the ~ 4 PeV knee of the all-particle spectra, such a result indicates

that the knee is dominated by nuclei heavier than Helium (Shibata et al. 2010; Zhao et al. 2015).

The direct measurements of lower energy CRs by balloon-borne or space detectors can determine the individual spectrum much better, which were then extrapolated to high energies to bridge the direct and air shower experiments (Hörandel 2003; Shibata et al. 2010; Zhao et al. 2015). The extrapolation was usually based on power-law fittings to the low energy data. However, remarkable spectral hardenings at a rigidity of a few hundred GV on the spectra of all major nuclei components were reported by the balloon-borne experiments ATIC-2 (Panov et al. 2007) and CREAM (Ahn et al. 2010), and were confirmed with higher precision by the space detectors PAMELA (Adriani et al. 2011) and AMS-02 (Aguilar et al. 2015b,a). Many kinds of models have been proposed to understand the origin of the spectral hardenings, including the super-position of different sources (Zatsepin & Sokolskaya 2006; Yuan et al. 2011; Thoudam & Hörandel 2012), the non-linear acceleration of the supernova remnant shocks (Biermann et al. 2010; Ptuskin et al. 2013), the re-acceleration mechanism when particles propagating in the Galaxy (Thoudam & Hörandel 2014), and the spatial-dependent diffusion of CRs (Tomassetti 2012; Gaggero et al. 2015; Jin et al. 2016; Tomassetti 2015; Guo et al. 2014, 2016).

Given these new measurements of both the direct and indirect experiments, we re-visit the “poly-gonato” model of CRs in this work. We tend to build an updated phenomenological model of the energy spectrum of each composition which matches these newest data. We adopt a log-parabolic spectrum with an asymptotically hardening spectral index of $\gamma + \beta \cdot \log E$ to describe the spectral hardenings. An exponential cutoff is employed to describe the knee of CRs. Through fitting to different data sets with the two key parameters, β and the cutoff energy E_c , we further test the consistency among

different measurements. As an illustration of a possible physical implementation of this “modified poly-gonato” model, we discuss a spatial-dependent diffusion model to reproduce the results of the phenomenological model.

2. “MODIFIED POLY-GONATO” MODEL

The “poly-gonato” model to describe the knee is basically based on the extrapolation of low-energy measurements. Up to the knee energies, typically three types of models were employed to fit the all particle spectrum. The first type is motivated by the diffusive shock acceleration or propagation process. In those models, the cutoff energies of CRs are expected to be proportional to the particle charge Z (Lagage & Cesarsky 1983; Ptuskin et al. 1993). The second type is motivated by interaction processes, in which the cutoff or break energies are proportional to the atomic number A (Karakula & Tkaczyk 1993; Kazanas & Nicolaidis 2001; Candia et al. 2002; Hu et al. 2009). The third type of the break is constant for all species. It is not well physically motivated, but might be a simple assumption (Hörandel 2003). Recent results show that the break energy of light components is lower than that of the all-particle knee, which disfavors this constant break energy scenario (Huang & for the Tibet AS γ Collaboration 2013; Mari et al. 2015; Bartoli et al. 2015b; D’Amone et al. 2015). Therefore, only the Z -dependent and A -dependent cases are considered in the following discussion.

To include the spectral hardenings at ~ 200 GV, we parameterize the spectrum of each composition as

$$\begin{aligned} \frac{d\Phi^i}{dE}(E) = & \Phi_0^i \times \left(\frac{E}{E_{\text{br}}} \right)^{-\gamma_1^i} \\ & \times \left(\frac{1 + (E/E_{\text{br}})^\delta}{2} \right)^{[\gamma_1^i - \gamma_2^i + \beta \cdot \log(E/\text{TeV})]/\delta} \\ & \times e^{-E/E_c^i}, \end{aligned} \quad (1)$$

where E_{br} is the break energy which describes the low energy (with a rigidity of a few GV) behavior of the spectrum, Φ_0^i is the absolute flux of the i th element at E_{br} , γ_1^i (γ_2^i) is the spectral index below (above) E_{br} , δ is a shape parameter which characterizes the sharpness of the low energy break, and $\beta \cdot \log(E/\text{TeV})$ is an asymptotically harder term used to describe the spectral hardening.

We find that for $E_{\text{br}}/Z = 4$ GV, $\gamma_1^i = 2.05$, and $\delta = 2.0$, the low energy spectra of most nuclei can be reasonably reproduced (see Figs. 1 and 3). Therefore they are fixed as above values for simplicity. For parameters γ_2^i and the flux normalizations, we fit the observational data for the major compositions. As for the parameters of other less abundant nuclei, we adopt the results given in Ref. ???. For convenience, these parameters are tabulated in the Appendix.

To account for the spectra around the knee, we assume Z - or A -dependent cutoff of each species as

$$E_c^i = \begin{cases} E_c^p \cdot Z, & \text{charge dependent} \\ E_c^p \cdot A, & \text{mass dependent} \end{cases} \quad (2)$$

where E_c^p is the cutoff energy of protons. Parameters E_c^p correlates with β . They will be determined through fitting to the data.

Eq. (1) has been used to fit the measured CR spectra for the major compositions, including p, He, C, O, Mg, Al, Si, and

TABLE 1
LOW ENERGY SPECTRAL PARAMETERS OF THE MAJOR COMPOSITIONS IN THE
“MODIFIED POLY-GONATO” MODEL

Z	Flux at TeV/n ($\text{m}^{-2}\text{s}^{-1}\text{sr}^{-1}\text{TeV}^{-1}$)	γ_2
1	7.51×10^{-2}	2.83
2	4.91×10^{-2}	2.76
6	9.12×10^{-3}	2.78
8	1.35×10^{-2}	2.80
12	5.17×10^{-3}	2.76
13	9.89×10^{-4}	2.78
14	6.85×10^{-3}	2.87
26	1.55×10^{-2}	2.71

Fe. The direct measurements of each species at low energies, e.g., by AMS-02 (Aguilar et al. 2015b,a), CREAM (Ahn et al. 2010), and HEAO-3 (Engelmann et al. 1990), as well as the air shower array measurements of the light components at high energies (Huang & for the Tibet AS γ Collaboration 2013; Mari et al. 2015; Bartoli et al. 2015b; Montini & Mari 2016) are used in the fitting. Due to the uncertainties of the absolute energy calibration and the hadronic interaction models of the ground based CR experiments, the observed break energies of the knee of light components differ from each other. According to these results, we classify the data into three groups, CREAM, Tibet experiments (AS γ , ARGO-YBJ and WFCTA), and KASCADE. The all-particle spectra are used to test different fittings. Fitting results of the spectral parameters are presented in Tables 1 and 2.

TABLE 2
HIGH ENERGY SPECTRAL PARAMETERS IN THE “MODIFIED POLY-GONATO” MODEL

	mode	CREAM	Tibet	KASCADE
β	Z	0.07	0.049	0.036
β	A	0.08	0.05	0.038
E_c^p	Z	0.42 PeV	1.3 PeV	4.2 PeV
E_c^p	A	0.21 PeV	0.65 PeV	2.1 PeV

Fig. 1 shows the fitting results for the Z -dependent scenario, compared with the data. In this figure, panels (a)-(c) are the spectra of protons, Helium, and p+He for the three groups corresponding to different data of the light component knee as described above. Panel (d) is for C and O, panel (e) is for Mg, Al, and Si, panel (f) is for Fe, respectively. Panels (g)-(i) are the all-particle spectra of the three groups.

We find that CREAM data prefers a relatively low energy knee of the light components, which under-shoots the all-particle spectra. The KASCADE data gives the highest energy of the knee, which slightly over-shoots, but is roughly consistent with, the all-particle spectra. The Tibet experimental data gives the best match with the all-particle one. In all these fittings, it seems that there is a tension between the CREAM data and the ground-based measurements. To better compare among different data sets, we show in Fig. 2 the 1σ (inner dashed) and 2σ (outer solid) contours on the $\beta - E_c^p$ plane. Other parameters are fixed to the values given in Table 2. We can see that at 2σ level, the CREAM favored parameter space does not overlap with those given by other data sets. The parameter regions for Tibet experiments, KASCADE, and the all-particle spectra are consistent with each other.

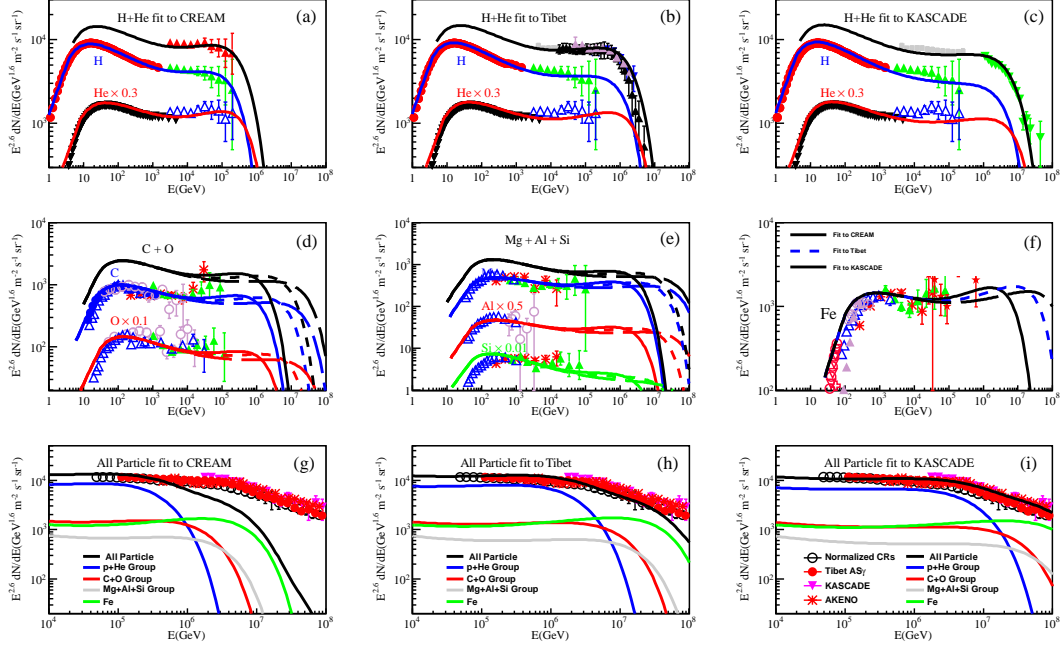


FIG. 1.— The comparison between the fitting results and the experimental data, for the Z-dependent case. The proton data are from: AMS-02 (Aguilar et al. 2015b), CREAM (Ahn et al. 2010), ATIC-2 (Panov et al. 2007); the Helium data are from: AMS-02 (Aguilar et al. 2015a), CREAM (Ahn et al. 2010); ATIC-2 (Panov et al. 2007); the Carbon, Oxygen, Magnesium, Aluminium, Silicon, and Iron data are from: HEAO-3 (Engelmann et al. 1990), the proton + Helium data are from: KASCADE (Apel et al. 2013), Tibet-AS γ (Huang & for the Tibet AS γ Collaboration 2013), WFCTA (Bartoli et al. 2015b), ARGO-YBJ (Mari et al. 2015; D’Amone et al. 2015); the all-particle data are from: Tibet-AS γ (Amenomori et al. 2008), KASCADE (Apel et al. 2013), Akeno (Nagano et al. 1984), and the normalized average one (Hörandel 2003).

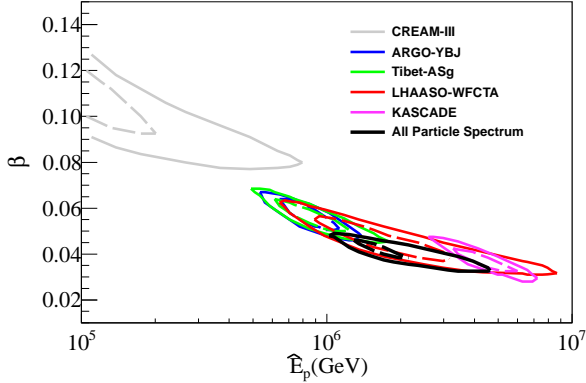


FIG. 2.— 68% (inner dashed) and 95% (outer solid) confidence regions of parameters β and E_p^P derived through fitting to the CREAM, ARGO-YBJ, AS γ , WFCTA, KASCADE, and the all-particle spectra.

The results for the A-dependent scenario are shown in Fig. 3. We have similar conclusion with that of the Z-dependent scenario. For the A-dependent case, the knee energy of protons is smaller by a factor of ~ 2 compared with that of the Z-dependent case. At present it is difficult to distinguish these two cases, and we need measurements of the knee of either protons or Helium to distinguish them.

3. THE SPATIAL-DEPENDENT DIFFUSION MODEL

In the above section, we introduce a “modified poly-gonato” model to reproduce the wide-band spectra of CRs. One possible physical explanation of the spectral hardening ($\beta \cdot \log E$) is the spatial-dependent diffusion of particles (Tomassetti 2012; Jin et al. 2016; Tomassetti 2015; Guo et al. 2016). In a simplified version, i.e., CRs diffuse separately in the disk region and halo region (the two-halo model), the

hardening of the primary CR nuclei and the excesses of secondary particles can be reasonably accounted for (Tomassetti 2012; Guo et al. 2016). Here we extrapolate this model to the knee region, to reproduce the results of the phenomenological “modified poly-gonato” model.

3.1. Model description

We employ the diffusion reacceleration model to describe the propagation of CR particles (see e.g., Strong et al. 2007). A cylindrical geometry is assumed. The propagation is confined in a halo with half height of z_h . The diffusion coefficient, D_{xx} , depends on both the spatial coordinates (r, z) and the particle rigidity, which is parameterized as (Guo et al. 2016)

$$D_{xx}(r, z, \rho) = \begin{cases} \eta(r, z) \beta \left(\frac{\rho}{\rho_0} \right)^{\varepsilon(r, z)}, & |z| < \xi z_h \text{ (disk)} \\ D_0 \beta \left(\frac{\rho}{\rho_0} \right)^{\delta_0}, & |z| > \xi z_h \text{ (halo)} \end{cases} \quad (3)$$

where β is the velocity of the particle in unit of light velocity c , D_0 represents the normalization of the halo diffusion coefficient at $\rho_0 = 4$ GV, δ_0 characterizes the rigidity dependence of the diffusion coefficient, ξz_h denotes the thickness of the disk, $\eta(r, z)$ and $\varepsilon(r, z)$ describes the spatial dependence of the diffusion coefficient in the disk. $\eta(r, z)$ and $\varepsilon(r, z)$ can be related to the source distribution $f(r)$, via a unified form as (Guo et al. 2016),

$$F(r, z) = \begin{cases} \left(\frac{1}{1 + e^{f(r)}} - A_i \right) [1 - (z/\xi z_h)^4] + F_0 \cdot (z/\xi z_h)^4 & \text{(disk)} \\ F_0 & \text{(halo)} \end{cases} \quad (4)$$

where A_i is a constant with i denoting η or ε , F_0 is the D_0 and δ_0 .

The reacceleration is described by a diffusion in the momentum space, with a relation between D_{pp} and D_{xx} as

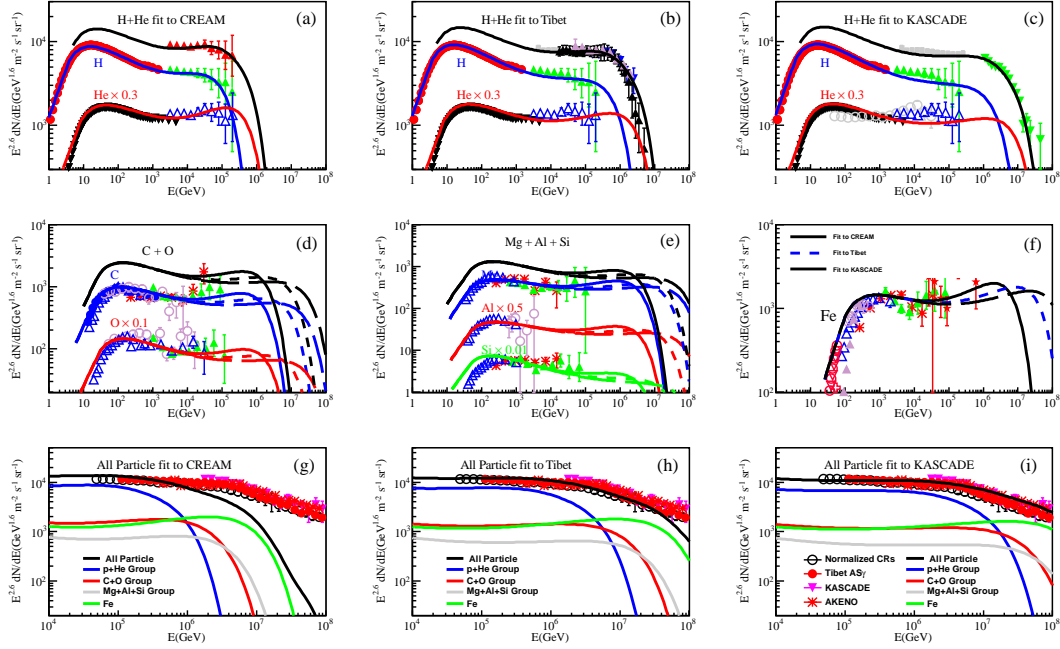


FIG. 3.— Same as Fig. 1 but for the A -dependent model.

(Seo & Ptuskin 1994)

$$D_{pp}D_{xx} = \frac{4p^2 v_A^2}{3\delta(4 - \delta^2)(4 - \delta)w}, \quad (5)$$

where p is the momentum of a particle, δ is the power-law index of the rigidity dependence of the spatial diffusion coefficient (see Eq. (3)), v_A is the Alfvén speed, w is the ratio of the magnetohydrodynamic wave energy density to the magnetic field energy density which is assumed to be 1.

The injection spectrum of CR nuclei is assumed to be broken power-law with an exponential cutoff

$$q_{\text{inj}}(E) = q_0 e^{-E/E_c} \times \begin{cases} (E/E_{\text{br}})^{-\gamma_1}, & E < E_{\text{br}} \\ (E/E_{\text{br}})^{-\gamma_2}, & E \geq E_{\text{br}} \end{cases} \quad (6)$$

where q_0 is the normalization factor, E_{br} is the break energy, γ_1, γ_2 are the spectral indices below and above E_{br} , and E_c characterizes the spectral cutoff around the knee. The relative abundances of different nuclei are adopted as the default values used in DRAGON Evoli et al. (2008). Similar as in Sec. 2, we consider either the Z -dependent and A -dependent models of the cutoff.

Low energy particles ($E \lesssim 10$ GeV/n) will be modulated by solar activities, showing suppress of their low energy fluxes. We use the force-field approximation to account for this solar modulation (Gleeson & Axford 1968). In this work, The modulation potential Φ is fixed to be 550 MV for all the nuclei except for B/C whose modulation potential is adopted as 200 MV.

3.2. Results

3.2.1. Primaries

We use the numerical code DRAGON to calculate the spatial dependent diffusion of CRs (Evoli et al. 2008). The injection spectral parameters are given in Tables 3. The parameter γ_2 differs for each species. They are tuned to fit the data for the major compositions. And for the less abundant nuclei, we

assume the same difference of γ_2 from that of protons as in Sec. 2. The full compilation of γ_2 are given in the Appendix.

The propagation parameters are given in Table 4. We perform fittings to the three data sets of the knee of the light components, as described in Sec. 2. Results of the primary CRs are shown in Figs. 4 and 5, for the Z - and A -dependent cutoff scenarios of the knee. We find that the results are very similar to that of the “modified poly-gonato” model fittings. It is shown that a log-parabolic shape of the energy spectrum is a good approximation of a class of models with smooth hardenings.

TABLE 3
INJECTION PARAMETERS IN THE “SPATIAL-DEPENDENT DIFFUSION” MODEL

mode	CREAM	Tibet	KASCADE
E_{br}	9.0 GV	9.0 GV	9.0 GV
γ_1	2.0	2.0	2.0
E_c^p	Z	0.4 PeV	2.0 PeV
E_c^p	A	0.2 PeV	0.9 PeV
		2.0 PeV	

TABLE 4
PROPAGATION PARAMETERS IN THE “SPATIAL-DEPENDENT DIFFUSION” MODEL

	CREAM	Tibet	KASCADE
D_0 (cm ² /s)	6.8×10^{28}	6.8×10^{28}	6.8×10^{28}
δ_0	0.58	0.52	0.5
v_A (km/s)	16	16	16
z_h (kpc)	5	5	5
ξ	0.128	0.116	0.106
A_η	0.10	0.10	0.10
A_ε	-0.17	-0.15	-0.14

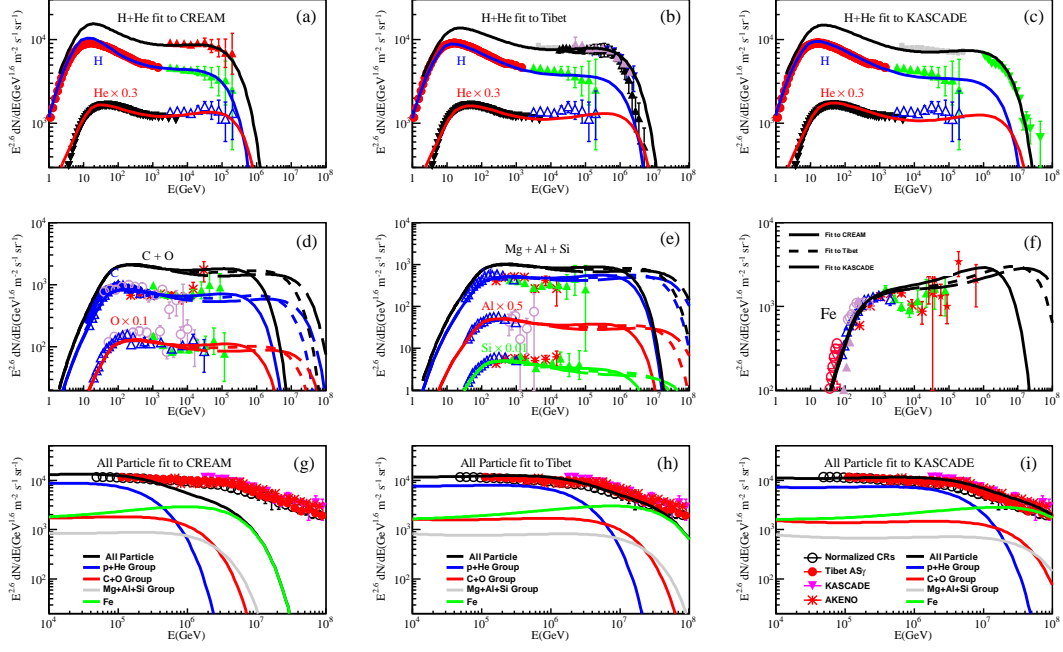


Fig. 4.— Same as Fig. 1, but for the spatial-dependent diffusion model.

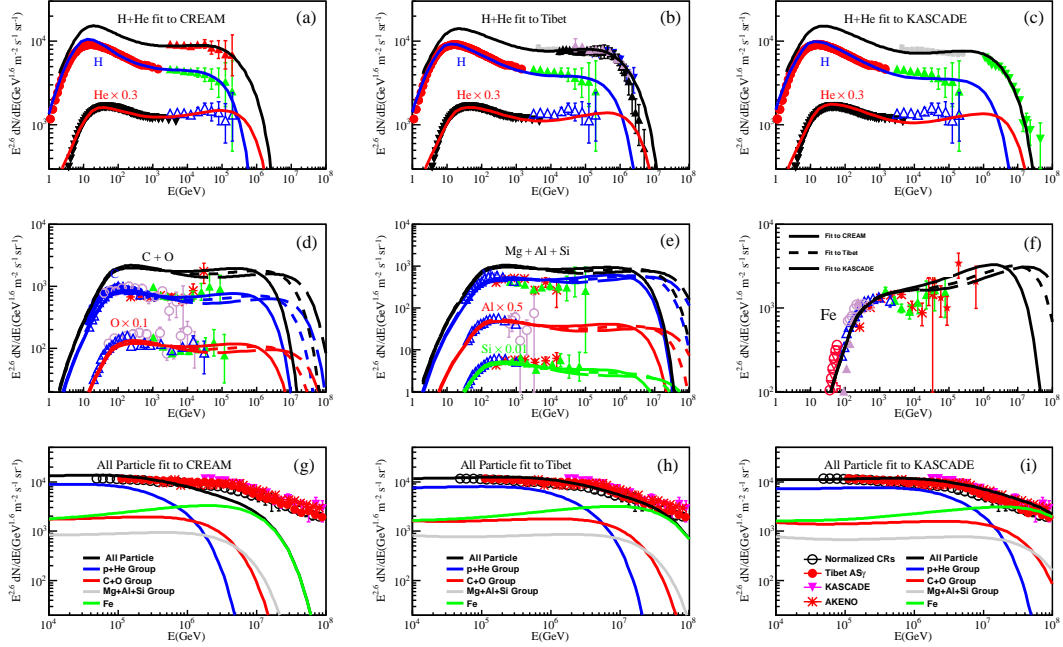


Fig. 5.— Same as Fig. 3, but for the spatial-dependent diffusion model.

3.2.2. Secondaries

Secondary particles will be produced by collisions of primary CRs with the interstellar medium when they propagate in the Galaxy. It is believed that most of antiprotons and Borons are such secondaries, which can be very effective to probe the particle propagation process. We calculate the expected \bar{p}/p and B/C ratios of this spatial-dependent diffusion model, as shown in Fig. 6. These results are reasonably consistent with the observational data. However, we do find that the second-to-primary ratio becomes asymptotically flatter at high energies, which is different from the simple uniform dif-

fusion scenario. This can be tested with future observations of the B/C ratio to higher energies.

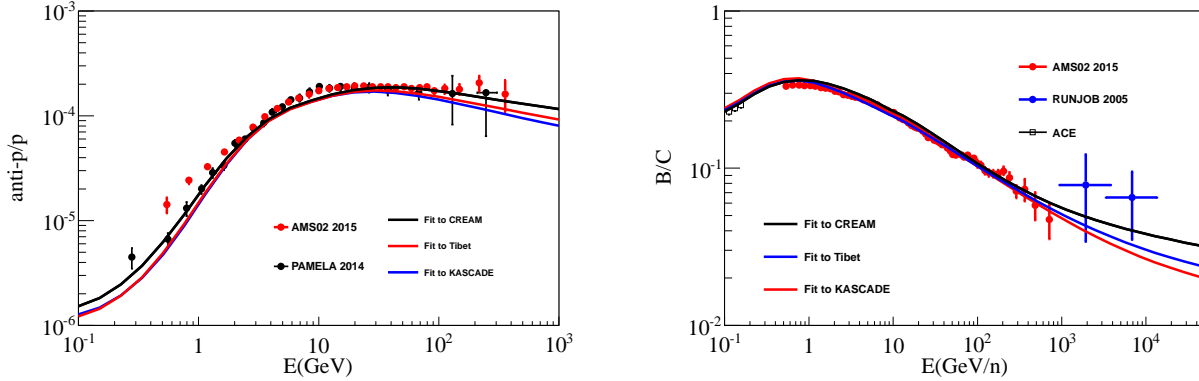


Fig. 6.— The calculated \bar{p}/p (left panel) and B/C (right panel) ratios of the spatial-dependent diffusion model. The \bar{p}/p data are from AMS-02 (AMS-02 collaboration 2015) and PAMELA (Adriani et al. 2014); the B/C data are from AMS-02 (AMS-02 collaboration 2015), ACE (Davis et al. 2000) and RUNJOB (Derbina et al. 2005).

3.2.3. Anisotropy

The flow of CRs will form a dipole anisotropy of arrival directions when observed at a fixed point. We calculate the amplitude of the dipole anisotropy of CRs as

$$A = \frac{D \nabla \phi}{c \phi}, \quad (7)$$

where ϕ is the locally observed differential fluxes of CRs. The dipole anisotropy amplitude as a function of energy is given in Fig. 7. The amplitude of the anisotropy is smaller than the prediction of the standard diffusion model (Tomassetti 2012; Guo et al. 2016), and is consistent with observations up to a few tens of TeV. Note, however, the phase of the observed anisotropy shows an evolution with energy, which can not be simply accounted for by the diffusion process (Amenomori 2015). More complicated process like the effect of the local magnetic field and/or local sources may be responsible for it (Ahlers 2016).

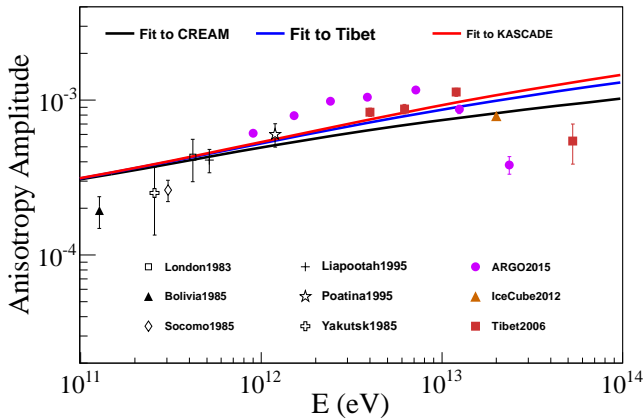


Fig. 7.— The calculated anisotropy of CRs for the spatial-dependent diffusion model. The data are from underground muon observations: London(1983) (Thambyahpillai 1983), Bolivia(1985)(Swinson & Nagashima 1985), Socorro(1985) (Swinson & Nagashima 1985), Yakutsk(1985) (Swinson & Nagashima 1985), Liapootah(1995) (Munakata et al. 1995), Poatina(1995) (Fenton et al. 1995) and air shower array experiments: Tibet(2006) (Amenomori et al. 2006), IceCube(2012) (Abbasi et al. 2012), ARGO-YBJ(2015) (Bartoli et al. 2015a).

4. CONCLUSION AND DISCUSSION

Recent observations revealed new features on the CR spectra, including spectral hardenings at ~ 300 GV rigidities from balloon or space detectors and the knee of light components (p and He) from air shower experiments. In this work we develop a modified version of the “poly-gonato” model of the knee, taking into account such new data. A log-parabolic term of the spectrum is employed to describe the spectral hardenings. As for the knee, we adopt an exponential cutoff spectrum to describe it, with the cutoff energy being proportional to Z or A of each species. We then fit the spectral parameters to the observational data. Due to the difficulty of the absolute energy calibration in the air shower experiments, the break positions of the light component spectra differ to some degree among different experiments. Therefore the fittings are done for three groups of data sets separately, based on the light component spectral measurements: CREAM, Tibet experiments (AS γ , WFCTA and ARGO-YBJ), and KASCADE.

We find that there seems to be a tension between the low energy measurement by CREAM and the high energy measurements by air shower experiments. The CREAM data imply too hard spectra of CRs to be consistent with the high energy data. We also find that the Tibet experiment and KASCADE data of light components are consistent with the all-particle data. Our “modified poly-gonato” model, with parameters determined through fitting to the Tibet experimental p+He data, gives the best match to all the data.

The discrepancy between CREAM and ground-based measurements is possibly due to experimental systematics. There are no good measurements in the energy range of 1 – 100 TeV. For example, the proton and Helium spectra by CREAM (Ahn et al. 2010) differ much from that by ATIC-2 (Panov et al. 2007). A direct comparison of the AMS-02 measured fluxes of Helium and that by CREAM shows that the CREAM ones are higher by about 20% at TeV/nucleon (Aguilar et al. 2015a). The spectrum measured by AMS-02 is also softer than that by CREAM. Further more precise measurements of the energy spectra of various species, by e.g., CALET (CALET Collaboration 2007), DAMPE (Chang 2014), and LHAASO (Cao 2010) will be very important to address this issue and better determine the model parameters.

Alternatively, it is possible that the fitting function, which basically has smooth behaviors of the hardening and cutoff, is not good enough to describe the data. If there are some sharp structures of the spectra, the tension may be alleviated.

However, in such a case the model may need fine tuning and may be less physical.

Finally we give a physical model with spatial-dependent diffusion of CRs to reproduce the results of this phenomenological “modified poly-gonato” model. Apart from the potential inconsistencies among different data sets, the energy spectra of the primary CRs, the secondary-to-primary ratios, and the amplitude of the anisotropy are shown to be consistent with observations. This model predicts asymptotical harden-

ing of the B/C ratio above hundreds of TeV/n, which can also be tested with future measurements.

ACKNOWLEDGMENTS

This work is supported by the National Key Program for Research and Development (No. 2016YFA0400200), and National Natural Science Foundation of China (Nos. 11135010, 11635011).

REFERENCES

- Abbasi, R., Abdou, Y., Abu-Zayyad, T., et al. 2012, *ApJ*, 746, 33
 Adriani, O., Barbarino, G. C., Bazilevskaya, G. A., et al. 2011, *Science*, 332, 69
 —. 2014, *Physics Reports*, 544, 323
 Aguilar, M., Aisa, D., Alpat, B., et al. 2015a, *Physical Review Letters*, 115, 211101
 —. 2015b, *Physical Review Letters*, 114, 171103
 Ahlers, M. 2016, *ArXiv e-prints*, arXiv:1605.06446
 Ahn, H. S., Allison, P., Bagliesi, M. G., et al. 2010, *ApJ*, 714, L89
 Amenomori, M., Ayabe, S., Bi, X. J., et al. 2006, *Science*, 314, 439
 Amenomori, M., Bi, X. J., Chen, D., et al. 2008, *ApJ*, 678, 1165
 Amenomori, M. e. a. 2015, *International Cosmic Ray Conference AMS-02 collaboration*. 2015, *Talks at the ‘AMS Days at CERN’*, 15-17 April
 Apel, W. D., Arteaga-Velázquez, J. C., Bakk, K., et al. 2013, *Astroparticle Physics*, 47, 54
 Bartoli, B., Bernardini, P., Bi, X. J., et al. 2015a, *ApJ*, 809, 90
 —. 2015b, *Phys. Rev. D*, 92, 092005
 Berezhko, E. G. 1996, *Astroparticle Physics*, 5, 367
 Biermann, P. L., Becker, J. K., Dreyer, J., et al. 2010, *ApJ*, 725, 184
 CALET Collaboration. 2007, *Nuclear Physics B Proceedings Supplements*, 166, 43
 Candia, J., Epele, L. N., & Roulet, E. 2002, *Astroparticle Physics*, 17, 23
 Cao, Z. 2010, *Chinese Physics C*, 34, 249
 Chang, J. 2014, *Chinese Journal of Space Science*, 34, 550
 D’Amone, A., De Mitri, I., & Surdo, A. 2015, *ArXiv e-prints*, arXiv:1502.04840
 Davis, A. J., Mewaldt, R. A., Binns, W. R., et al. 2000, in *American Institute of Physics Conference Series*, Vol. 528, *Acceleration and Transport of Energetic Particles Observed in the Heliosphere*, ed. R. A. Mewaldt, J. R. Jokipii, M. A. Lee, E. Möbius, & T. H. Zurbuchen, 421–424
 Derbina, V. A., Galkin, V. I., Hareyama, M., et al. 2005, *ApJ*, 628, L41
 Engelmann, J. J., Ferrando, P., Soutoul, A., Goret, P., & Juliusson, E. 1990, *A&A*, 233, 96
 Evoli, C., Gaggero, D., Grasso, D., & Maccione, L. 2008, *Journal of Cosmology and Astroparticle Physics*, 10, 18
 Fenton, K. B., Fenton, A. G., & Humble, J. E. 1995, *International Cosmic Ray Conference*, 4, 635
 Gaggero, D., Grasso, D., Marinelli, A., Urbano, A., & Valli, M. 2015, *ArXiv e-prints*, arXiv:1504.00227
 Gleeson, L. J., & Axford, W. I. 1968, *ApJ*, 154, 1011
 Guo, Y.-Q., Feng, Z.-Y., Yuan, Q., Liu, C., & Hu, H.-B. 2013, *New Journal of Physics*, 15, 013053
 Guo, Y. Q., Hu, H. B., & Tian, Z. 2014, *ArXiv e-prints*, arXiv:1412.8590
 Guo, Y.-Q., Tian, Z., & Jin, C. 2016, *ApJ*, 819, 54
 Hörandel, J. R. 2003, *Astroparticle Physics*, 19, 193
 —. 2004, *Astroparticle Physics*, 21, 241
 Hu, H.-B., Yuan, Q., Wang, B., et al. 2009, *ApJ*, 700, L170
 Huang, J., & for the Tibet AS γ Collaboration. 2013, *International Cosmic Ray Conference*
 Jin, C., Guo, Y.-Q., & Hu, H.-B. 2016, *Chinese Physics C*, 40, 015101
 Karakula, S., & Tkaczyk, W. 1993, *Astroparticle Physics*, 1, 229
 Kazanas, D., & Nicolaidis, A. 2001, *International Cosmic Ray Conference*, 5, 1760
 Kulikov, G. V., & Kristiansen, G. B. 1958, *J. Exp. Theor. Phys.*, 35, 635
 Lagage, P. O., & Cesarsky, C. J. 1983, *A&A*, 125, 249
 Mari, S. M., Montini, P., & for the ARGO-YBJ Collaboration. 2015, *ArXiv e-prints*, arXiv:1502.01894
 Montini, P., & Mari, S. M. 2016, *ArXiv e-prints*, arXiv:1608.01389
 Munakata, K., Yasue, S., Mori, S., et al. 1995, *International Cosmic Ray Conference*, 4, 639
 Nagano, M., Hara, T., Hatano, Y., et al. 1984, *Journal of Physics G Nuclear Physics*, 10, 1295
 Panov, A. D., Adams, Jr., J. H., Ahn, H. S., et al. 2007, *Bulletin of the Russian Academy of Science, Phys.*, 71, 494
 Ptuskin, V., Zirakashvili, V., & Seo, E.-S. 2013, *ApJ*, 763, 47
 Ptuskin, V. S., Rogovaya, S. I., Zirakashvili, V. N., et al. 1993, *A&A*, 268, 726
 Seo, E. S., & Ptuskin, V. S. 1994, *ApJ*, 431, 705
 Shibata, M., Katayose, Y., Huang, J., & Chen, D. 2010, *ApJ*, 716, 1076
 Strong, A. W., Moskalenko, I. V., & Ptuskin, V. S. 2007, *Annual Review of Nuclear and Particle Science*, 57, 285
 Swinson, D. B., & Nagashima, K. 1985, *Planet. Space Sci.*, 33, 1069
 Thambyahpillai, T. 1983, *International Cosmic Ray Conference*, 3, 383
 Thoudam, S., & Hörandel, J. R. 2012, *MNRAS*, 421, 1209
 —. 2014, *A&A*, 567, A33
 Tomassetti, N. 2012, *ApJ*, 752, L13
 —. 2015, *Phys. Rev. D*, 92, 063001
 Voelk, H. J., & Biermann, P. L. 1988, *ApJ*, 333, L65
 Wang, B., Yuan, Q., Fan, C., et al. 2010, *Science China Physics, Mechanics, and Astronomy*, 53, 842
 Wiebel-Sooth, B., Biermann, P. L., & Meyer, H. 1998, *A&A*, 330, 389
 Yuan, Q., Zhang, B., & Bi, X.-J. 2011, *Phys. Rev. D*, 84, 043002
 Zatsepin, V. I., & Sokolskaya, N. V. 2006, *A&A*, 458, 1
 Zhao, Y., Jia, H.-Y., & Zhu, F.-R. 2015, *Chinese Physics C*, 39, 125001

APPENDIX

We present the spectral parameters of all nuclei up to Iron as used in this work.

TABLE 5
LOW ENERGY SPECTRAL PARAMETERS OF ALL NUCLEI IN THE “MODIFIED POLY-GONATO” MODEL (SEC. 2).

Symbol	Z	Flux at TeV/n ($\text{m}^{-2}\text{s}^{-1}\text{sr}^{-1}\text{TeV}^{-1}$)	γ_2
H	1	7.51×10^{-2}	2.83
He	2	4.91×10^{-2}	2.76
Li	3	1.78×10^{-3}	2.66
Be	4	4.07×10^{-4}	2.87
B	5	7.70×10^{-4}	3.07
C	6	9.12×10^{-3}	2.78
N	7	2.02×10^{-3}	2.84
O	8	1.35×10^{-2}	2.80
F	9	2.82×10^{-4}	2.81
Ne	10	3.95×10^{-3}	2.76
Na	11	6.48×10^{-4}	2.78
Mg	12	5.17×10^{-3}	2.76
Al	13	9.89×10^{-4}	2.78
Si	14	6.85×10^{-3}	2.87
P	15	2.32×10^{-4}	2.81
S	16	1.97×10^{-3}	2.67
Cl	17	2.52×10^{-4}	2.80
Ar	18	7.19×10^{-4}	2.76
K	19	4.60×10^{-4}	2.77
Ca	20	1.26×10^{-3}	2.82
Sc	21	2.61×10^{-4}	2.76
Ti	22	9.80×10^{-4}	2.73
V	23	5.43×10^{-4}	2.75
Cr	24	1.17×10^{-3}	2.79
Mu	25	1.16×10^{-3}	2.58
Fe	26	1.55×10^{-2}	2.71

TABLE 6
INJECTION SPECTRAL PARAMETERS γ_2 OF ALL NUCLEI IN THE “SPATIAL-DEPENDENT DIFFUSION” MODEL (SEC. 3).

Symbol	Z	γ_2
H	1	2.43
He	2	2.36
Li	3	2.26
Be	4	2.47
B	5	2.67
C	6	2.38
N	7	2.44
O	8	2.40
F	9	2.41
Ne	10	2.36
Na	11	2.38
Mg	12	2.36
Al	13	2.38
Si	14	2.47
P	15	2.41
S	16	2.27
Cl	17	2.40
Ar	18	2.36
K	19	2.37
Ca	20	2.42
Sc	21	2.36
Ti	22	2.33
V	23	2.35
Cr	24	2.39
Mu	25	2.18
Fe	26	2.31